

From FA Smith, Applied Radiation Physics

10.4 Diagnostic Radiology (DR)

This is the name given to conventional X-ray imaging in which the photon energies are sufficiently low to make photoelectric effect the dominant interaction. Anode potentials are generally 100 kVp or less. The image is then formed as a result of differential absorption in tissue volumes having different mean atomic numbers (Z).

Fig.(10.12) shows a typical arrangement for reflection geometry.

The spectrum of X-rays that emerges from an X-ray tube is polyenergetic because :

- X-ray production takes place at all energies between the anode potential and zero as the electron de-accelerates in the target,
- X-rays produced at different depths within the target receive different amounts of attenuation within the target material itself. This is called self-absorption.
- X-rays emerge into ambient air either through a thinned portion of the glass envelope or through a thin beryllium window. These produce a certain amount of inherent filtration. Additional filtration can then be added according to the requirements of the object being radiographed.

Transmitted X-rays can be detected either by film or in real-time.

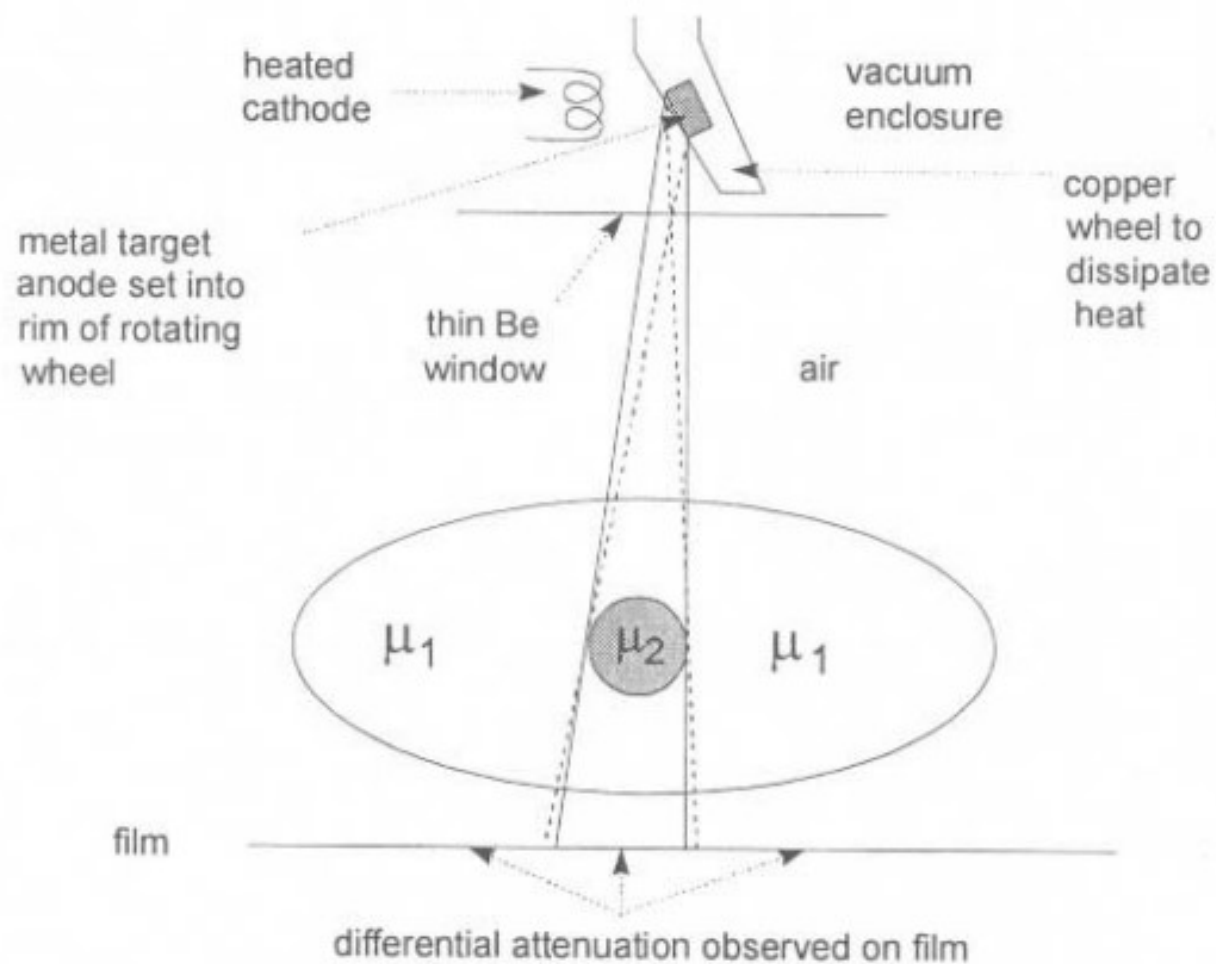


Fig.(10.12) A schematic diagram of image production on a film detector due to differential attenuation of a polyenergetic X-ray beam by a body containing regions of different attenuation coefficients μ_1 and μ_2 .

10.4.1 Film

X-ray film is similar to optical film in which microcrystals of silver bromide are dispersed in a gelatin matrix. The main differences are that in a nuclear emulsion the grains sizes are smaller ($\sim 0.1 - 0.6 \mu\text{m}$ compared with $\sim 1 - 3.5 \mu\text{m}$ in an optical emulsion) and their concentration by weight higher ($\sim 80\%$ compared with $\sim 50\%$) [1]. The speed of the film is determined by the distribution of grain sizes – the larger the range of sizes the faster the film [2].

On exposure to radiation, the silver in the AgBr grains is converted to elemental silver to form a latent image. Although the concentration of silver at this stage is too small to be visible, these Ag seeds enhance the production of much greater quantities of silver when the film is developed.

The larger the amount of radiation received by the film, the larger the number of seeds in the latent image and the larger will be the final amount of silver when the film is developed. Areas of the film having the higher concentration of silver will appear more opaque i.e. they will have a higher optical density (O.D).

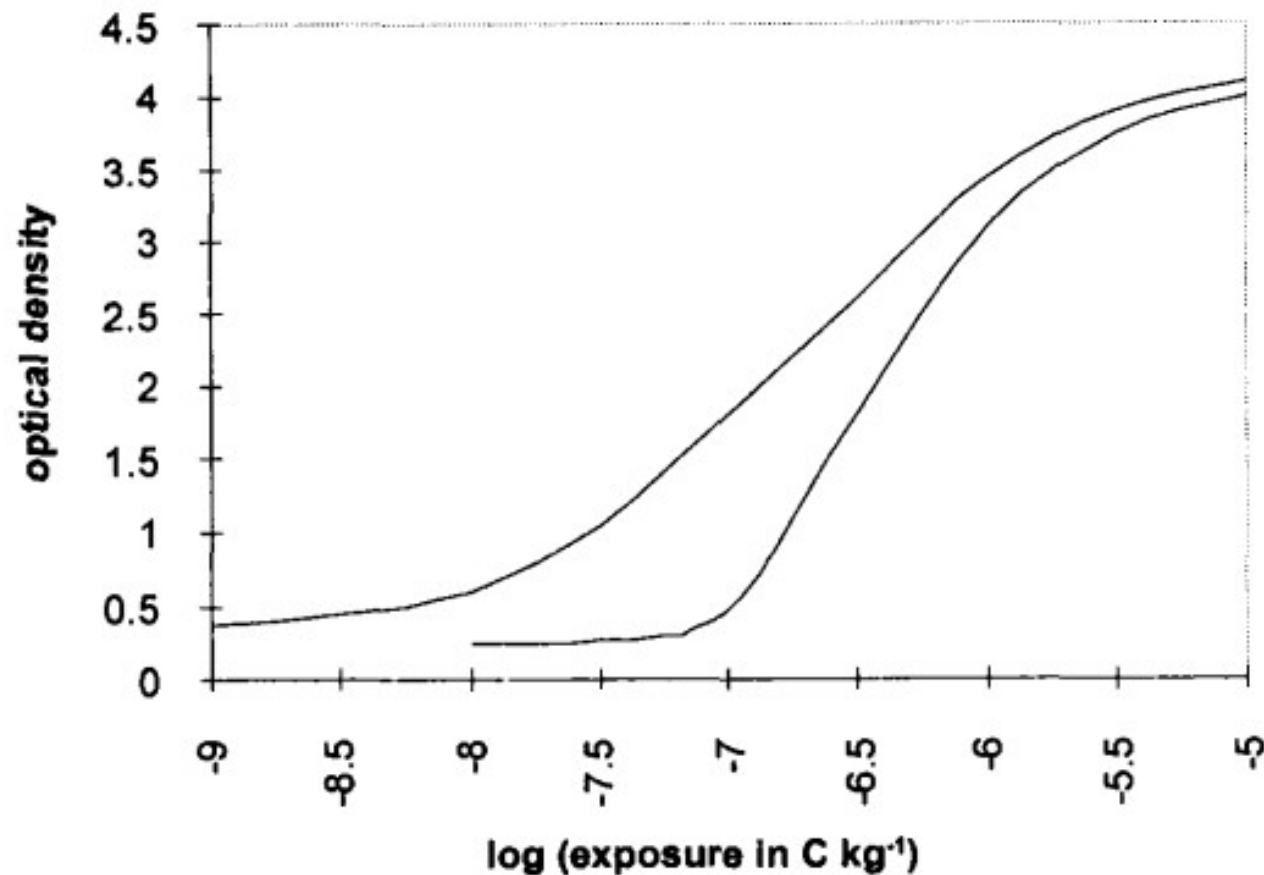


Fig.(10.13) Characteristic curves of typical radiographic films. The left hand curve corresponds to the faster film because it produces an optical density of unity at the lower exposure. It has a wider distribution of grain diameters which accompanies a larger mean grain diameter. This produces a smaller film Γ . The relative speed of the two films at OD = 1 is approximately 7. The values of the film Γ are 1.8 (left hand) and 3.4 (right hand). The latitudes are approximately 3×10^{-8} to 10^{-6} C kg⁻¹ (left hand) and 2×10^{-7} to 10^{-6} C kg⁻¹ (right hand).

It must be remembered that the AgBr grains in a film will be converted to elemental silver even without the initial presence of a latent image. The process of conversion is faster, however, when the latent image is present. Hence the importance of the developing time to achieve the optimum contrast between regions of different optical density.

Each nuclear emulsion has its own characteristic curve of optical density versus logarithm of exposure as shown in Figs.(10.4) and (10.13). A given film is distinguished by :

- the maximum slope, called the film Γ ,
- the range of exposures over which the curve is quasi-linear, called the latitude,
- the range of optical density between the fogging level and the saturation density,
- the speed (or sensitivity). This is the reciprocal of the exposure necessary to produce a given optical density (usually O.D. = 1).

The Optical Density of a film is defined as :

$$O.D = \log_{10} \left(\frac{I_0}{I} \right)$$

where I is the intensity of white light transmitted through the film when I_0 is the incident intensity. The Film Γ gives the maximum Contrast and is defined as :

$$\Gamma = \frac{OD_1 - OD_2}{\log(E_1) - \log(E_2)} \quad (10.2)$$

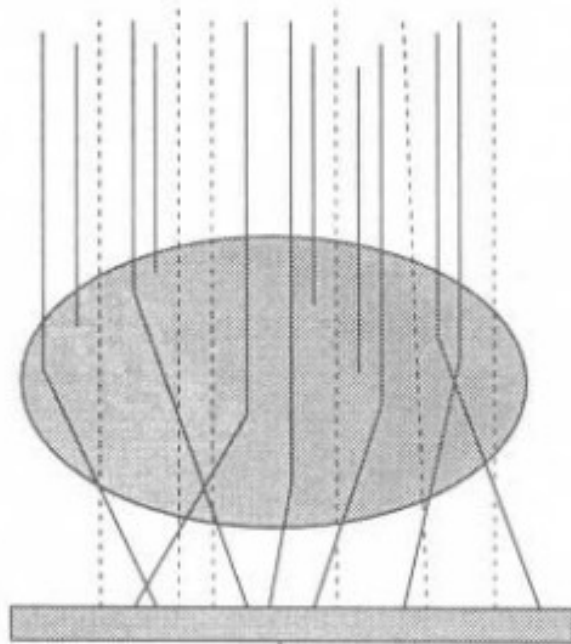
where E_1 and E_2 are X-ray exposures.

10.4.2 Reduction of contrast due to scatter

Although the photoelectric effect is the interaction of importance in diagnostic radiology, scatter cannot be ignored since it reduces contrast on a radiographic film (Fig.10.14).

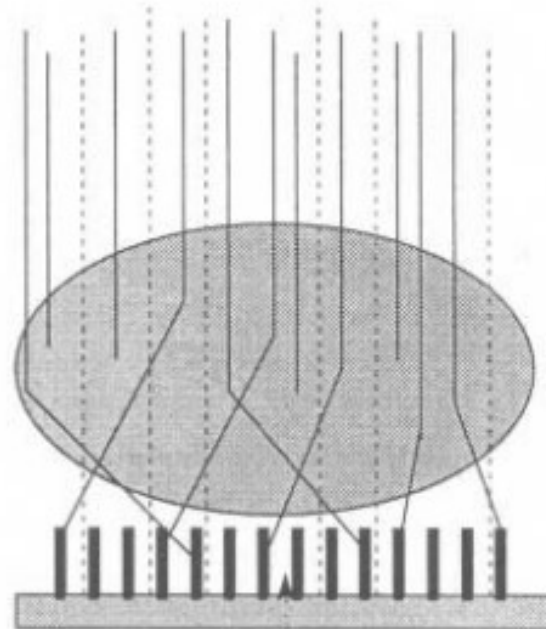
The contribution of scattered photons will tend to be uniformly distributed across the detector face. Two neighbouring regions on the detected image which are due to differences in photoelectric absorption will therefore both have the same scatter background. Table (10.2) uses Fig.(10.13) to illustrate the effect of adding a constant scatter background of $2.46 \times 10^{-8} \text{ C kg}^{-1}$ to two features on an image having optical densities 1.1 and 2.25 in the absence of any scatter. The presence of scatter reduces the contrast from 1.15 to 0.95 – a reduction of 17%.

(a)



film or film/screen
combination alone

(b)



reduction of scatter
component due to
insertion of grid

Fig.(10.14) The reduction of scattered photons received on a radiographic detector can be achieved by, (a) minimizing the distance between the detector and the object, and (b) by interposing a grid between the object and the detector. In each diagram, 4 photons have interacted by the photoelectric effect and have stopped in the object, 7 photons have scattered and 6 photons have not interacted in the object at all, and have reached the film without any deviation.

Table (10.2) Reduction in contrast between two features when an additional scatter component of $2.46 \times 10^{-8} \text{ C kg}^{-1}$ reaches the radiographic film in Fig.(10.13).

no scatter			with added scatter		
OD	log E	E (C kg ⁻¹)	E (C kg ⁻¹)	log E	OD
1.1	-7.5	3.16×10^{-8}	5.62×10^{-8}	-7.25	1.4
2.25	-6.75	1.78×10^{-7}	2.03×10^{-7}	-6.69	2.35

10.4.3 Intensifying screens

The sensitivity of a film can be increased by converting some of the incident X-ray photons into optical photons to which the film is more sensitive. This is achieved by means of a fluorescent material, in close contact with the emulsion layer, with the following properties :

- It must have a high Z in order to maximize its absorption in the low energy region where the photoelectric effect is dominant.
- It must possess a high quantum efficiency to emit a large number of optical photons at a wavelength which matches the optical absorption spectrum of the emulsion.
- The fluorescence should have a short lifetime so that there is no significant afterglow.

Screens can be intensifying (for normal radiography employing cassettes) or fluorescence (for real-time observation). The emission characteristics of the two types are slightly different since emulsion sensitivity generally peaks near 400 nm while the sensitivity of the human eye is greatest in the green – yellow region of the optical spectrum (~ 550 nm).

Thus, calcium tungstate and zinc sulphide (which peak ~ 430 nm) are used in intensifying screens while zinc cadmium sulphide (peaking near 550 nm) is a typical material used for fluorescence screens. The conversion is determined by the quantum efficiency :

$$QE = \frac{N_o h\nu_o}{N_x h\nu_x} \quad (10.3)$$

where N_o and N_x are the numbers of optical and x-ray photons at frequencies of ν_o and ν_x respectively.

Since fluorescence emission is isotropic, it produces a smearing about the sharpest edge, the consequences of which are illustrated in Figs.(10.5) and (10.6). The effect of a screen on the overall resolution is therefore to reduce the MTF considerably.

10.4.4 Real-time detectors for X-ray imaging

Fluoroscopy replaces the film+intensifying screen combination with a fluorescence screen. Until the advent of television monitors and image intensifiers, this had to be viewed directly by the radiologist in a darkened room. This is no longer necessary, however, now that electronic amplification of the image is possible. The principle of the image intensifier makes use of two fluorescence screens and an electron acceleration section, Fig.(10.15) :

- X-rays emerging from the patient, as in Fig.(10.15), strike the input fluorescence screen.
- The input screen emits optical photons over its characteristic emission spectrum. This must match as closely as possible the spectral sensitivity of a photocathode screen with which it is placed in immediate contact. (A scintillation crystal is matched to its photocathode in the same way, see Chapter 5).

material to the photocathode in the same way, see Chapter 5).

- Electrons emitted from the photocathode are accelerated through electron lenses while retaining the relative spatial positions of the input optical photons. These electrons strike the output fluorescence screen where they produce optical photons more efficiently due to their higher energy. A brighter image is the result.
- The isotropic nature of fluorescence emission requires that a thin layer of aluminium be placed on the photocathode side of the output screen to prevent photons from interacting again with the photocathode. If this were to happen, further electron generation would take place and create a uniform background at the output. Contrast would thereby be reduced.

The development of solid-state detector technology has opened up new possibilities in the use of digital image formation. Two main approaches are being followed. The first converts the X-ray image into optical photons and then into charge. The second converts the X-rays directly into charge. Charge images are produced in both cases and these can then be read out electronically. Examples of work in this area are :

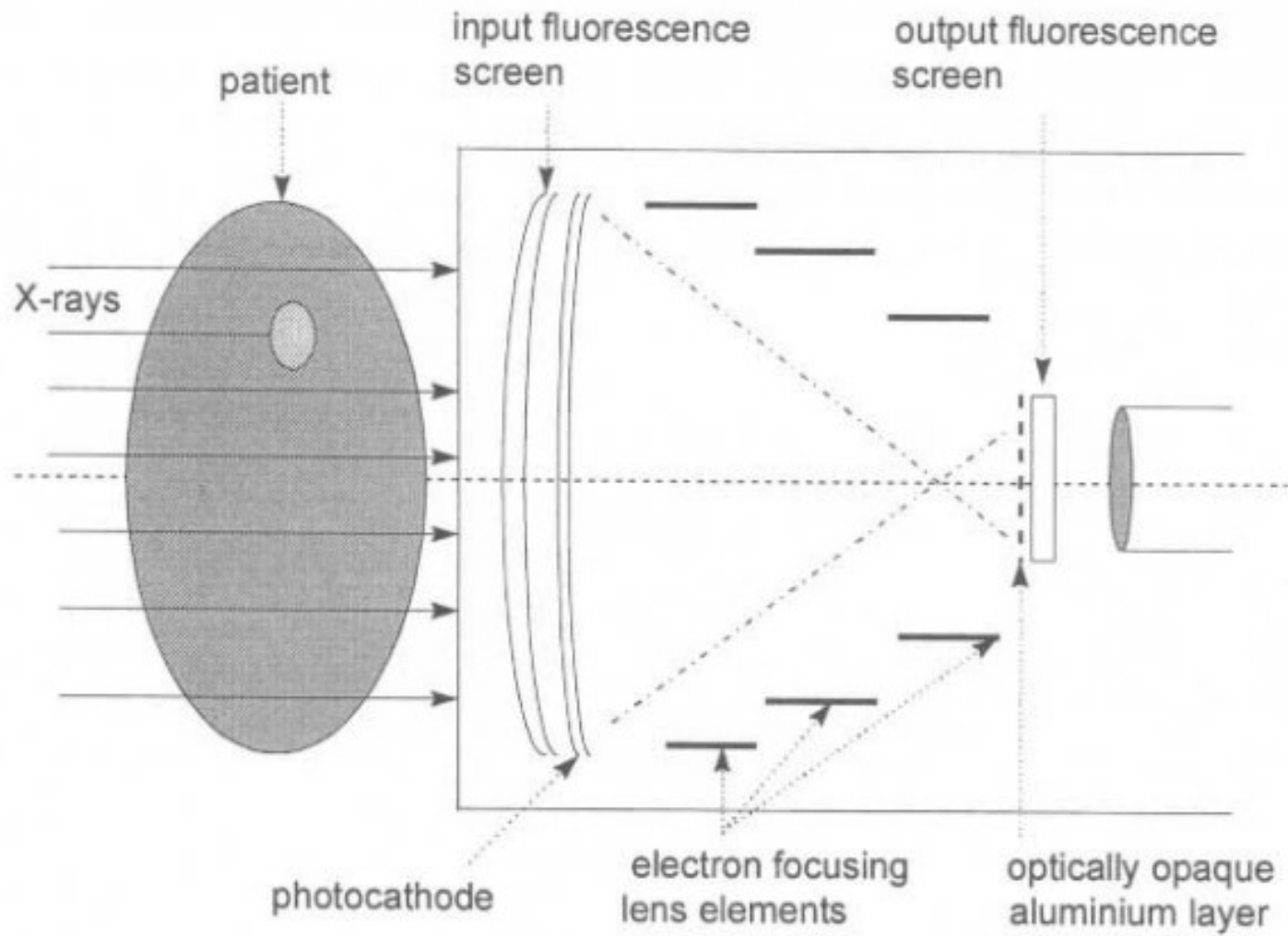


Fig.(10.15) A schematic diagram of an image intensifier.

The conversion of X-rays first into optical photons and then into charge. For low energy X-rays, as in mammography, a phosphor-coated charge-coupled detector (CCD) has been used [3]. The CCD device is coated with a 100 μm thick layer of $\text{Gd}_2\text{O}_2\text{S}:\text{Eu}$ scintillator screen (GadOx) directly onto the surface of the electrodes, Fig.(5.29a). This scintillator has a peak optical emission (630 nm) which matches the spectral response of the CCD. At molybdenum K_α energies, (17.4 keV, see Table (10.1)), the scintillator has $\sim 92\%$ attenuation of X-rays giving a peak signal of $\sim 4 \times 10^6$ electrons per pixel. The resolution is slightly better than a conventional film+screen mammography combination. For an MTF of 0.7 the CCD system can resolve ~ 2.8 line pairs/mm compared with 2.2 line pairs/mm for the film+screen combination [3]. Amorphous silicon together with a metal plate/scintillation screen combination has also been developed for use in portal imaging [4].

- the direct conversion of an X-ray image into charge using amorphous selenium [5],[6],[7],[8]. For the direct conversion of X-rays into charge, a photoconductive layer of amorphous selenium is deposited onto an active matrix array of thin-film transistors. The latter comprises an array of CdSe transistors with a 160 μm pixel pitch onto which is evaporated a 300 μm layer of amorphous selenium. A thin indium layer is evaporated on the top of the selenium to provide the high voltage bias. In this case, however, the X-ray image is converted directly into a charge image which is then read out in real-time using the active matrix. A resolving capability of ~ 3.3 line pairs/mm was measured at an MTF of 0.7 [6].

10.5 Computerized Tomography (CT)

The principle of CT is shown in Fig.(10.16). A narrow beam of X-rays is rotated about the long axis of the patient and transmitted photons are recorded at each angular position. Count rate information of the type illustrated in Fig.(10.16) is then reconstructed to give a 2-dimensional map of attenuation coefficient over the whole transaxial slice.

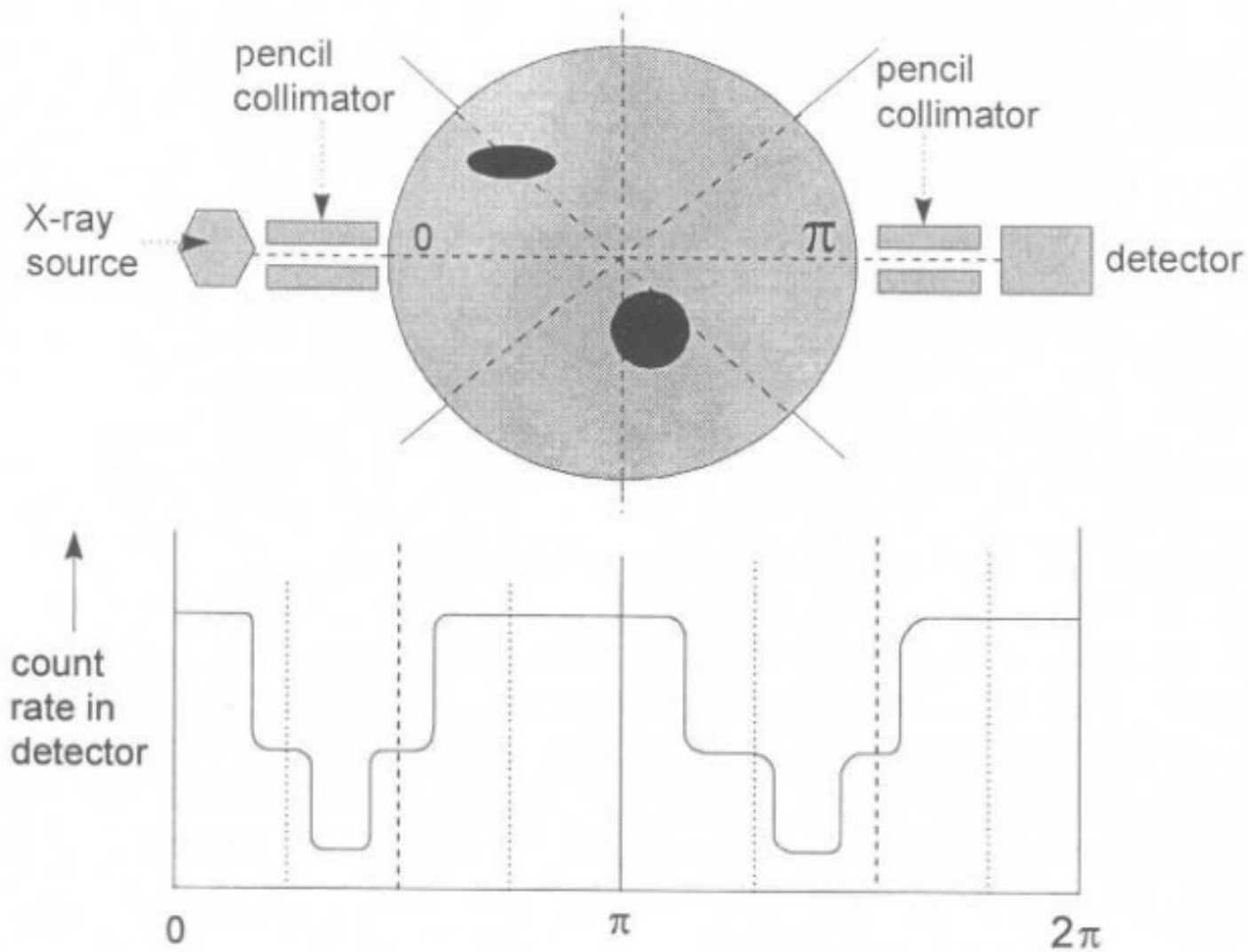


Fig.(10.16) Arrangement of X-ray Computed Tomography system. Regions of high attenuation are indicated in black. The X-ray source/detector combination in this example gives approximate count rates versus angle as shown.

The object of a CT scan is to determine a difference in attenuation coefficient between neighbouring regions of tissue. Reference is made to water since this is the major component in human body tissue. Thus, a CT number is defined for each pixel of the scan :

$$\text{CT number} = \frac{\mu_{\text{tissue}} - \mu_{\text{water}}}{\mu_{\text{water}}} \quad (10.4)$$

Fig.(10.17) Linear attenuation coefficients versus photon energy for typical body tissues [9].
Average Adult Soft Tissue (ICRU 33): ◆ photoelectric absorption, ■ Compton.
Adult Cortical Bone: ▲ photoelectric absorption, ✕ Compton.

Detectors in a CT scanner are real-time solid state devices with a much higher detection efficiency than radiographic film. It is necessary to increase the mean photon energy in order to :

- maximize transmission through the patient. Counting statistics are mainly responsible for limiting the precision with which the CT number can be determined.
- reduce patient dose. The price paid for the great improvements in image quality is the large number of exposures required. A higher photon energy corresponds to lower attenuation coefficients in order to give less dose per exposure.

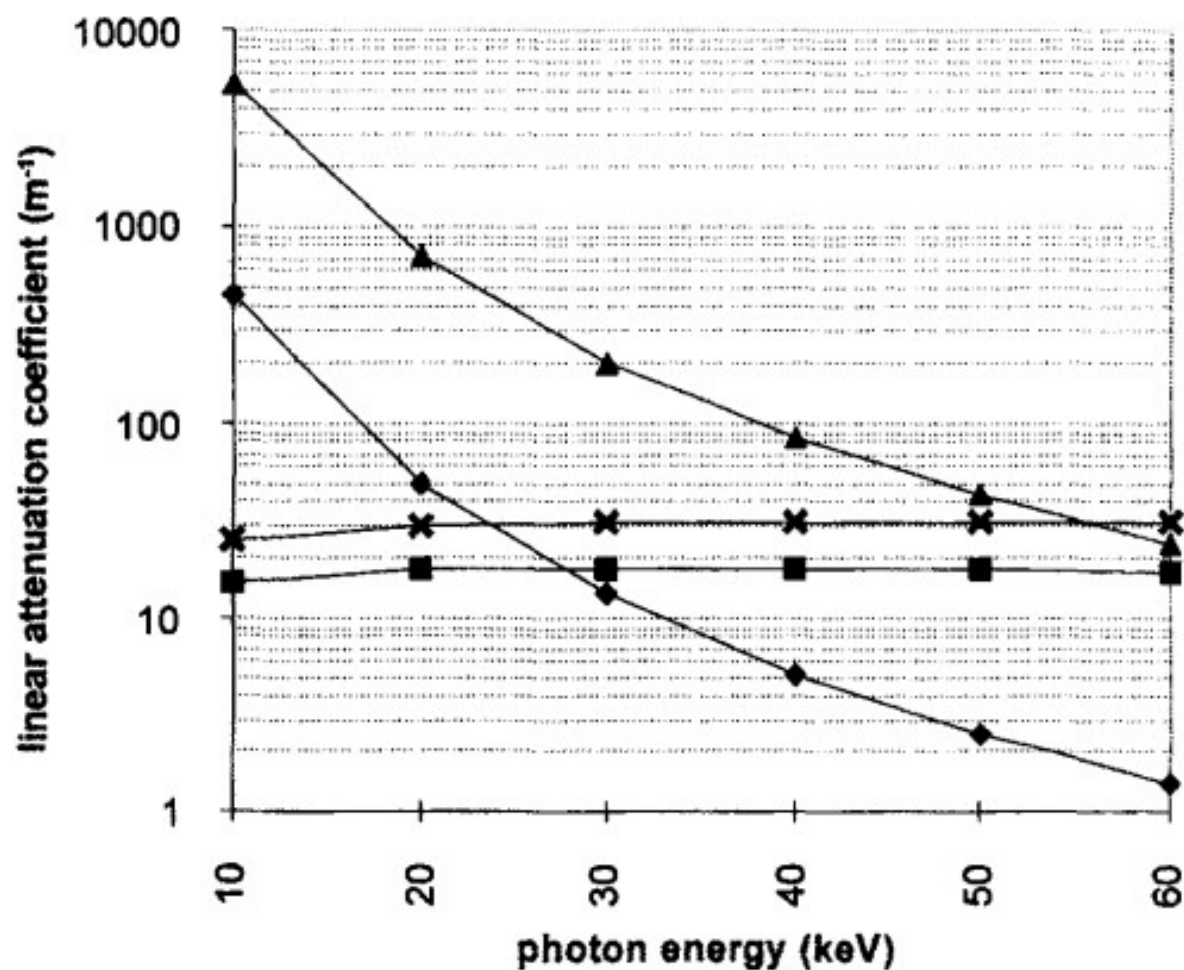


Fig.(10.17) Linear attenuation coefficients versus photon energy for typical body tissues [9].
 Average Adult Soft Tissue (ICRU 33): ♦ photoelectric absorption, ■ Compton.
 Adult Cortical Bone: ▲ photoelectric absorption, ✕ Compton.

Fig.(10.17) gives the linear attenuation coefficients for average soft tissue and adult cortical bone [9]. Depending upon the examination, conventional diagnostic radiology uses tube voltages in the approximate range 30 – 80 kVp. The mean photon energies therefore lie in the approximate range 15 – 30 kV over which the photoelectric effect is dominant. Tube voltages in CT, however, vary in the range 120 – 140 kVp. Fig.(10.17) shows that at a mean energy near 40 kV, it is Compton interactions that are now the most probable. As a consequence, CT images represent tissue density, and not atomic number, since all tissues contain the same number of electrons per kg to within $\sim 5\%$.

10.5.1 Spatial resolution

A determination of the resolving capability of a CT scanner is made from an initial measurement of a point spread function (PSF) or a line spread function (LSF). As in any other branch of medical physics, quality assurance demands that protocols are followed in the setting-up of equipment for use on patients. For this purpose, test objects containing a number of features of differing size and contrast are used. The measurement of a line spread function, for example, would use a test object as shown in Fig.(10.18).

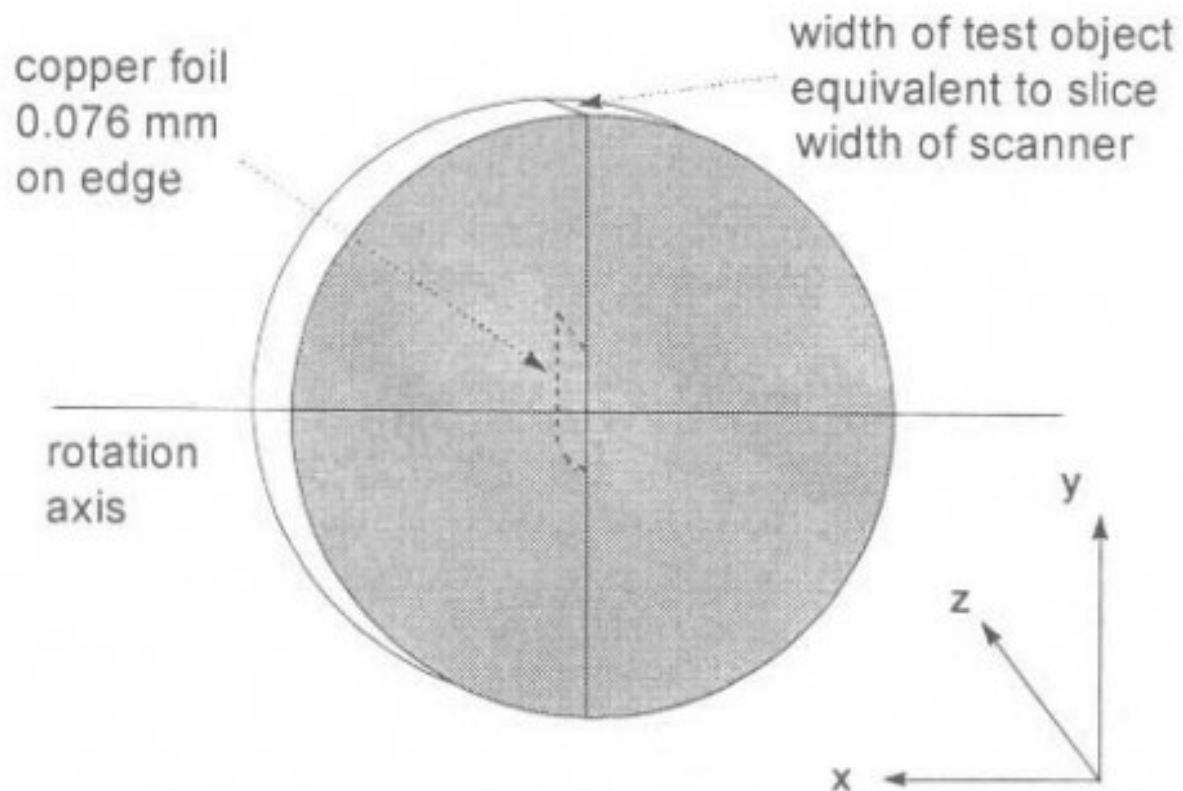


Fig.(10.18) A Line Spread Function test object [10]. A thin copper foil (0.076 mm) is placed at the centre of a disc of Perspex (PMMA) of diameter 20 cm and thickness 1.5 – 2.5 cm.

A disc of Perspex, with thickness equivalent to the slice width of the scanner, (~ 10 mm) is mounted in the plane of the detectors. The 0.076 mm thick copper foil, with a width equal to that of the Perspex disc, is orientated vertically across the central rotation axis. So long as the orientation of the copper foil is orthogonal to the pixel rows along the x-axis, interpolation between the measured points gives the point spread function. The Fourier transform of the PSF, as carried out in section 10.2.2, gives the MTF.

A very much simpler method of finding the MTF can be followed under the assumption that the PSF is Gaussian [11]. It was established that this is indeed the case for five widely-used scanners. Earlier work [12] had shown that when a

generalized PSF, $f(x,y)$, is simplified for radial symmetry, $f(r)$, the MTF at spatial frequency ν can be written :

$$MTF(\nu) = \frac{\left| \int_0^{\infty} f(r) j(2\pi\nu r) r dr \right|}{\int_0^{\infty} f(r) r dr} \quad (10.5)$$

where $j = \sqrt{-1}$. With the assumption of a Gaussian PSF we have :

$$PSF(r) = f(r) = e^{-\alpha^2(r-\varepsilon)^2} \quad (10.6)$$

In Eq.(10.6) ε is the displacement of the centre of the PSF with respect to the origin of the co-ordinate system of the CT pixels, and α is related to the FWHM of the PSF by $\alpha = 1.665/\text{FWHM}$. Substituting Eq.(10.6) into Eq.(10.5) and integrating [13] gives :

$$MTF(\nu) = e^{-(\pi\nu/10\alpha)^2} \quad (10.7)$$

In Eq.(10.7) the factor 10 appears when the FWHM is measured in mm so that α has units of mm^{-1} . Spatial frequency ν is given in line pairs cm^{-1} .

10.5.2 Contrast

Discrimination between low contrast objects is limited largely by the amplitude and frequency characteristics of noise in the detector system. Again, it is determined for a given system by scanning a test object, as in Fig.(10.18), in which the copper foil is replaced by thin foils of plastic having graded sizes and densities.

Subject contrast, SC, between two neighbouring regions of an image is related to the differences in attenuation coefficients, as in Eq.(10.4). Thus :

$$SC = \frac{k}{\mu_w(E)} [\mu_1(E) - \mu_2(E)] \quad (10.8)$$

where k is the CT scaling constant ($k = 1000$) and the subscripts on the linear attenuation coefficients refer to water and regions 1 and 2 of the image. Assuming that the attenuation coefficients 1 and 2 differ from that of water by a constant which is energy independent, and that regions 1 and 2 are identical in composition but differ only in density, the subject contrast can be written [10] :

$$SC = \frac{k}{\mu_w(E)} \frac{\mu_1(E)}{\rho_1} [\rho_1 - \rho_2] \quad (10.9)$$

10.5.3 Radiation dose

Radiation dose must be considered from the point of view of both the patient and the operating personnel. Scanner manufacturers should supply data on normalized scatter air kerma rates, measured along the central axis of the machine, at 1m distance from the centre of the detector plane. Together with this data, iso-exposure curves should also be given in plan view and in vertical elevation [10]. Typical values for normalized scatter air kerma rates at 1m for machines in current use lie in the range 0.7×10^{-3} to 3.8×10^{-3} mGy mA⁻¹ min⁻¹.

Fourth generation scanners have a stationary ring of detectors within which the X-ray tube rotates in a concentric path. With anode voltages in the range 120 – 140 kVp, each scan is further specified by :

- The product of tube current (mA) and the time of the scan (s) in mAs.
- The slice width. This is generally 10 mm but it can be as small as 5 mm for brain scans.
- The pitch. This is the separation of the contiguous slices. The pitch is unity when the separation between slices is equal to the slice width.

In the UK, the NRPB publish guidelines on the determinations of total effective dose and organ dose for different scans [14]. Together with the lower figures for the latest technique in helical scanning, these are shown in Table (10.3) for representative scanners, and compared with figures for conventional diagnostic radiology (DR) for similar examinations.

Table (10.3) A comparison of representative doses for four types of X-ray examinations. All doses are given in mSv. Figures in columns 2 and 4 come from [14]. Figures in columns 5,6 and 7 come from the comparison between a typical 4th Generation CT scanner and a helical CT scanner.

Exam	DR	Organ with max dose	CT Effective Dose	CT Organ Dose	Helical Effective Dose	Helical Organ Dose
Brain	0.2	Brain	3.5	45.9	0.7	20.0
Chest	0.05	Thymus	9.1	39.1	2.2	9.8
Abdomen	1.4	Kidney	8.8	38.7	2.1	9.1
Pelvis	1.2	Bladder	9.4	39.9	2.4	9.5

Considerably lower patient doses are achieved by the use of helical scanning

(HCT). Here there is a continuous movement of the patient at a constant speed through the detector plane. This reduces the time during which no data is taken to practically zero, and is a significant improvement on the step-wise scan-movement-scan-movement sequence of the 4th generation scanners. Doses given in columns 5, 6 and 7 in Table (10.3) show a large reduction in both overall effective dose as well in organ doses when a pitch of 1.3 is used in HCT. In this case the movement of the patient through the detector plane is 30% faster than in non-helical scanning. Just some of the many additional complexities of image reconstruction which arise in HCT are treated in [15],[16] and [17].